Concentrated Bone Marrow Aspirate Improves Full-Thickness Cartilage Repair Compared with Microfracture in the Equine Model

By Lisa A. Fortier, DVM, PhD, Hollis G. Potter, MD, Ellen J. Rickey, DVM, Lauren V. Schnabel, DVM, Li Foong Foo, MD, Leroy R. Chong, MD, Tracy Stokol, BVSc, PhD, Jon Cheetham, VetMB, PhD, and Alan J. Nixon, BVSc, MS

Investigation performed at Cornell University College of Veterinary Medicine, Ithaca, and the Hospital for Special Surgery, New York, NY

Background: The purpose of this study was to compare the outcomes of treatment with bone marrow aspirate concentrate, a simple, one-step, autogenous, and arthroscopically applicable method, with the outcomes of microfracture with regard to the repair of full-thickness cartilage defects in an equine model.

Methods: Extensive (15-mm-diameter) full-thickness cartilage defects were created on the lateral trochlear ridge of the femur in twelve horses. Bone marrow was aspirated from the sternum and centrifuged to generate the bone marrow concentrate. The defects were treated with bone marrow concentrate and microfracture or with microfracture alone. Second-look arthroscopy was performed at three months, and the horses were killed at eight months. Repair was assessed with use of macroscopic and histological scoring systems as well as with quantitative magnetic resonance imaging.

Results: No adverse reactions due to the microfracture or the bone marrow concentrate were observed. At eight months, macroscopic scores (mean and standard error of the mean, 9.4 ± 1.2 compared with 4.4 ± 1.2; $p = 0.009$) and histological scores (11.1 ± 1.6 compared with 6.4 ± 1.2; $p = 0.02$) indicated improvement in the repair tissue in the bone marrow concentrate group compared with that in the microfracture group. All scoring systems and magnetic resonance imaging data indicated that delivery of the bone marrow concentrate resulted in increased fill of the defects and improved integration of repair tissue into surrounding normal cartilage. In addition, there was greater type-II collagen content and improved orientation of the collagen as well as significantly more glycosaminoglycan in the bone marrow concentrate-treated defects than in the microfracture-treated defects.

Conclusions: Delivery of bone marrow concentrate can result in healing of acute full-thickness cartilage defects that is superior to that after microfracture alone in an equine model.

Clinical Relevance: Delivery of bone marrow concentrate to cartilage defects has the clinical potential to improve cartilage healing, providing a simple, cost-effective, arthroscopically applicable, and clinically effective approach for cartilage repair.

Focal chondral or osteochondral defects have been identified in 61% to 67% of knee arthroscopy procedures[1-3]. Several operative procedures have been used to enhance cartilage repair in an attempt to diminish knee pain, restore joint function, and delay the development of osteoarthritis. Techniques ranging from debridement and/or microfracture to methods including implantation of synthetic materials or scaffolds with or without cells have been developed and used for cartilage repair[3]. The authors of a systematic review of Level-I and II studies involving 421 patients treated with autologous chondrocyte implantation, osteochondral autograft transfer, matrix-induced autologous chondrocyte implantation, or microfracture, and followed for a mean of 1.7 years, concluded that no technique consistently yielded superior results and that all studies showed improvement in clinical outcome measures in all treatment groups as compared with the preoperative findings[4].

Although these techniques present options to the surgeon, the development of a single-step, simple, autogenous, cost-effective cartilage repair procedure would be ideal. Furthermore, an optimal procedure would be one that could be applied arthroscopically to minimize morbidity and that could provide cells for chondrogenesis, growth factors to enhance matrix synthesis, and a scaffold to retain the cells within the defect and protect the neocartilaginous tissue[5,6]. Microfracture fits many of these criteria and is effective at relieving pain in the short term (for less than twenty-four months). However, the repair tissue lacks normal cartilage matrix structure, and the long-term durability of the repair tissue has been called into question[4,7,8]. The goal of this study was to determine the capacity of a concentrated bone marrow aspirate to achieve repair of large, full-thickness cartilage defects. Our hypothesis was that bone marrow concentrate would enhance cartilage repair compared with that following microfracture.

Bone marrow aspirate has been investigated as a source of mesenchymal stem cells for regeneration of cartilage and other tissues of the musculoskeletal system[9-12]. In bone marrow aspirates, mesenchymal stem cells represent a very small fraction of the total population of nucleated cells[13]. Studies suggest that 0.001% to 0.01% of mononuclear cells, after density gradient centrifugation of the bone marrow aspirate to remove red blood cells, granulocytes, immature myeloid precursors, and platelets, are mesenchymal stem cells[13,14]. The number of mesenchymal stem cells can be increased through culture expansion, but then the technique is no longer a simple, one-step method of tissue regeneration.

Bone marrow aspirate is also a rich source of growth factors, including platelet-derived growth factor (PDGF), transforming growth factor-β (TGF-β), and vascular endothelial growth factor (VEGF)[15,16]. These growth factors are contained within the alpha-granules of platelets and are secreted by mesenchymal stem cells[17,18]. The chondrogenic effects of these growth factors on mesenchymal stem cells have been investigated, and studies have suggested that combinations of growth factors are important for inducing effective chondrogenesis[11,19,20].

The importance of a three-dimensional environment to facilitate mesenchymal stem-cell chondrogenesis is well documented[21,22]. The use of either platelet-rich plasma or fibrin clots as biologically based three-dimensional scaffolds enhances mesenchymal stem-cell chondrogenesis in vitro compared with that observed in traditional three-dimensional pellet culture systems[23-25]. Both platelet-rich plasma and fibrin clots are typically generated with use of peripheral blood plasma and thrombin-mediated cleavage of fibrinogen to fibrin, and the same biological mechanism can be utilized to clot bone marrow concentrate and generate three-dimensional constructs in situ.

The objective of this study was to evaluate treatment with bone marrow concentrate as a method to repair large full-thickness cartilage defects. Our hypothesis was that bone marrow concentrate with microfracture would significantly improve the quality and quantity of repair tissue compared with that achieved with microfracture alone.

Materials and Methods

Experimental Design and Study Population

This project was approved and performed according to guidelines of the Institutional Animal Care and Use Committee. Twelve mixed-breed, young adult horses (two to five years of age; mean body weight, 425 kg) were used. The animals were considered to be free of patellofemoral joint abnormalities on the basis of physical examination, lameness examination, and patellofemoral radiographs. Prior to surgery, computer-generated assignments were used to designate whether the left or right limb of each horse was to receive bone marrow concentrate and microfracture or microfracture alone.

Surgical Procedures

Preoperative and postoperative antibiotics and a nonsteroidal anti-inflammatory agent were administered. Caudal epidural analgesia was also administered preoperatively to minimize postoperative pain[26]. The horses were anesthetized and placed in dorsal recumbency, and 70 mL of bone marrow was aspirated from the sternum prior to the initiation of arthroscopic surgery. The bone marrow was aspirated from two sternal marrow spaces (with 35 mL aspirated from each) into syringes containing preservative-free heparin to a final concentration of 15 U of preservative-free heparin/mL of bone marrow aspirate. The contents of the two syringes were mixed together to obtain one homogeneous sample of bone marrow aspirate, and an aliquot was removed for cytological analyses and flow cytometry. The bone marrow aspirate (60 mL) was placed into a bone marrow aspirate concentrate (BMAC) disposable (Harvest Technologies, Plymouth, Massachusetts) and processed in a SmartPReP 2 centrifuge (Harvest Technologies) to yield 6 mL of bone marrow concentrate. One milliliter was retained for cytological analyses and flow cytometry, and the remainder was reserved for surgical application.

An arthroscope was then inserted sequentially into each patellofemoral joint. The articulations were explored to rule out any preexisting cartilage lesions. A 15-mm-diameter custom-made guarded spade-bit cutter, premeasured to drill 3 mm deep, was introduced into the joint through a second portal and used to create a single full-thickness cartilage defect in the lateral trochlear ridge of each femur approximately 2 cm distal to the apex of the patella. Any remaining calcified cartilage was removed with a surgical curet. The fluid medium used for initial arthroscopic maneuvers was replaced by sterile helium gas, and the subchondral bed of the cartilage lesion was dried by suction and insertion of several lint-free sponges. An awl was used to create six microfracture sites, placed approximately 6 mm apart. For the defects to be treated with the bone marrow concentrate, bone marrow concentrate and thrombin (10:1 volume ratio) were mixed on injection into the defect with use of a mixing syringe and injected until the bone marrow concentrate was flush with the surrounding host cartilage. The thrombin was resuspended in, and activated with, 10% $CaCl_2$ to achieve a final concentration of 1000 U/mL. The contralateral, control limb was treated with microfracture alone. The joints were irrigated with fluid to remove residual gas and

moved through a range of motion to verify that the bone marrow concentrate grafts remained positioned within the defect.

Following surgery, the horses were confined to box-stall rest for two weeks and then allowed ten minutes of walking exercise daily, which increased each week. Second-look arthroscopy was performed at twelve weeks after surgery. Repair tissue was scored with use of the International Cartilage Repair Society (ICRS) macroscopic scoring system[27-29]. No biopsies were performed. The horses were killed at eight months after the initial surgery, and the knee joints were removed for 3-T quantitative magnetic resonance imaging[30-36] and histological analyses. The histological findings were scored with the ICRS system[37].

Cytological and Flow Cytometry Analysis

All samples (bone marrow aspirate and bone marrow concentrate) for cytological analysis and flow cytometry were evaluated in a blinded fashion by a board-certified veterinary clinical pathologist (T.S.). Routine clinical cytological analysis of bone marrow aspirate and bone marrow concentrate was performed to determine the platelet count, red blood-cell count, packed red blood-cell volume, white blood-cell count, and myeloid:erythroid ratio. Fold changes in cytological categories were calculated from bone marrow aspirate and bone marrow concentrate values.

Flow cytometry was performed on the samples of bone marrow aspirate and bone marrow concentrate, but only the results from the samples of bone marrow concentrate were available as a result of the low number of nucleated cells in the bone marrow aspirate. Flow cytometry was performed, as previously described, with a FACSCalibur flow cytometer (BD Biosciences, San Jose, California) equipped with a 488-μm argon laser and BD CellQuest analysis software (BD Biosciences)[38,39]. Cells were assessed for immunoreaction against antibodies to CD45 (VMRD, Pullman, Washington), CD44 (AbD Serotech, Raleigh, North Carolina), CD34 (BD Biosciences, San Jose, California), CD29 (BD Biosciences), and CD172a (AbD Serotech). These markers were chosen on the basis of the previous literature, which suggests that mesenchymal stem cells are negative for CD45 and CD34 and positive for CD29, CD44, and CD172a[13,40].

Imaging

Magnetic resonance imaging of the patellofemoral joint was conducted on a 3-T clinical system (GE Healthcare, Milwaukee, Wisconsin) with use of an eight-channel knee coil (Invivo, Orlando, Florida). Morphological imaging was performed with use of cartilage-sensitive fast-spin-echo sequences in sagittal and axial planes through the trochlea with the following parameters: repetition time = 3500 to 6000 msec, echo time = 25 to 35 msec, echo train length = twelve to thirteen, at three excitations with a maximum resolution of 253 μm × 253 μm × 1.5 mm. Receiver bandwidth was 62.5 kHz over the entire frequency range. The morphological pulse sequence has been used previously in preclinical models and has been assessed for accuracy with use of histological findings as the standard[32,41].

T1ρ-weighted images were acquired with use of a spin-lock technique and three-dimensional spoiled gradient-recalled (3D SPGR) acquisition, with use of a magnetization-prepared, angle-modulated, partitioned k-space snapshot technique[42]. T2 mapping was performed with use of a multislice, multiecho modified Carr-Purcell-Meiboom-Gill (CPMG) pulse sequence, which utilizes interleaved slices and tailored refocusing pulses to minimize contribution from stimulated echoes[43]. Both quantitative pulse sequences were performed in the axial plane, with use of a multislice, multiecho technique, with a repetition time of 800 msec and eight echoes sampled (8 to 64 msec). Quantitative T1ρ mapping was performed with use of a repetition time of 2000 msec; a field of view of 13 cm; a slice thickness of 2.5 cm; a matrix of 4096 × 12; a time of spin-lock of 20, 40, 60, 80 msec; eight excitations; and a spin-lock frequency of 500 Hz.

Standardized regions of interest for quantitative T1ρ and T2 mapping included tissue in the central part of the defect, in the peripheral part of the defect, in the interface between the defect and the surrounding host tissue, adjacent to the defect (1 cm from the periphery of the defect), and remote from the defect (medial trochlear tissue). In each region of interest, T1ρ mapping and T2 mapping were performed separately in the superficial and deep halves of the respective tissues, with care taken to not include the synovial fluid or the subchondral plate, respectively, as well as to avoid sampling at the magic angle. Fast-spin-echo acquisitions were used to determine the Outerbridge score[44], the percent fill of the defect with repair tissue as determined by a review of both the coronal and the sagittal images (providing a tomographic assessment of the fill of the defect by thirds: 0% to 33%, 34% to 66%, and 67% to 100%[32]), the presence of subchondral bone overgrowth, the extent of sclerosis, and the synovial reaction.

Gross and Histological Processing and Scoring

All scoring was performed by two independent evaluators (L.A.F. and E.J.R.), who were blinded to the treatment group. Subsequent to magnetic resonance imaging, the joints were opened and photographed. Gross specimens were assessed with use of the ICRS macroscopic scoring system on a scale of 12 to 0, with 12 being normal and indistinguishable from the surrounding articular cartilage[27]. Synovial membrane and osteochondral sections were obtained for histological analysis, fixed in 4% paraformaldehyde, embedded in paraffin, and sectioned at 8 μm. Osteochondral sections were decalcified in cacodylate-buffered 10% EDTA prior to embedding. Sections were stained with hematoxylin and eosin for ICRS histological scoring[37], stained with safranin O and fast green to indicate proteoglycan content and distribution[45], and processed for type-II collagen immunochemistry. Synovial membrane sections were assessed for villous architecture, subintimal fibrosis, intimal cellular thickening, vascularity, and inflammatory cell infiltrate on a scale of 15 to 0, with 15 being normal. Osteochondral histological sections were scored with use of the ICRS scoring system on a scale of 18 to 0, with 18 being normal[37].

TABLE I Results of Cytological Analysis of Bone Marrow Aspirate and Bone Marrow Concentrate

	Bone Marrow Aspirate*	Bone Marrow Concentrate*	Absolute Change*	Relative Change†	P Value
Platelet count ($\times 10^3/\mu L$)	31.1 ± 21.2	208.3 ± 192.4	177 ± 183	8.7 (3.6-13.7)	0.002
White blood-cell count ($\times 10^3/\mu L$)	36.54 ± 16.6	267 ± 213	230 ± 207	7.4 (4.1-10.7)	0.0007
Red blood-cell count ($\times 10^3/\mu L$)	6774 ± 2060	3156 ± 1665	−3617 ± 2065	0.52 (0.35-0.69)	<0.0001
Packed red blood-cell volume (%)	31.7 ± 5	17.3 ± 11.4	−14.3 ± 12.1	0.55 (0.34-0.76)	0.0004
Myeloid-to-erythroid ratio	1.84 ± 0.85	2.09 ± 1.46	0.25 ± 1.03	1.13 (0.78-1.47)	0.36

*The values are presented as the mean and standard deviation. N = 10. †The relative change is presented as the mean with the 95% confidence interval in parentheses.

Statistical Methods

A paired t test was used to compare cytological data from the bone marrow aspirate specimens with that from the bone marrow concentrate specimens. Flow cytometry data were considered descriptive and therefore not subjected to statistical analysis. For all other outcome measures, a mixed-effect model (with horse as a random effect) was fitted to the data, including arthroscopic scores at twelve weeks postoperatively, gross and histological scores after the animal was killed, and magnetic resonance imaging data. The magnetic resonance imaging data were assessed to determine percentage fill, synovial reaction, subchondral bone reaction, and Outerbridge score. Quantitative magnetic resonance imaging datasets were analyzed with use of a linear least-squares estimation (FuncTool 3.1; GE Healthcare). T2 and T1ρ values were recorded from superficial and deep tissues within the five standardized regions of interest as described in the Materials and Methods section. Significance was set at p ≤ 0.05.

Results

Surgical Implantation and Clinical Evaluation

The bone marrow concentrate was easily delivered to all joints to form a clot level with the surrounding host cartilage (Fig. 1). In one animal, the bone marrow concentrate clot became dislodged while the joint was moved through a range of motion after the bone marrow concentrate injection, and it was visualized arthroscopically. The clot was removed from the patellofemoral joint, the base of the defect was dried, another clot was injected, and it remained in place during a subsequent range of motion. One animal was killed immediately postoperatively because spinal cord damage sustained during recovery
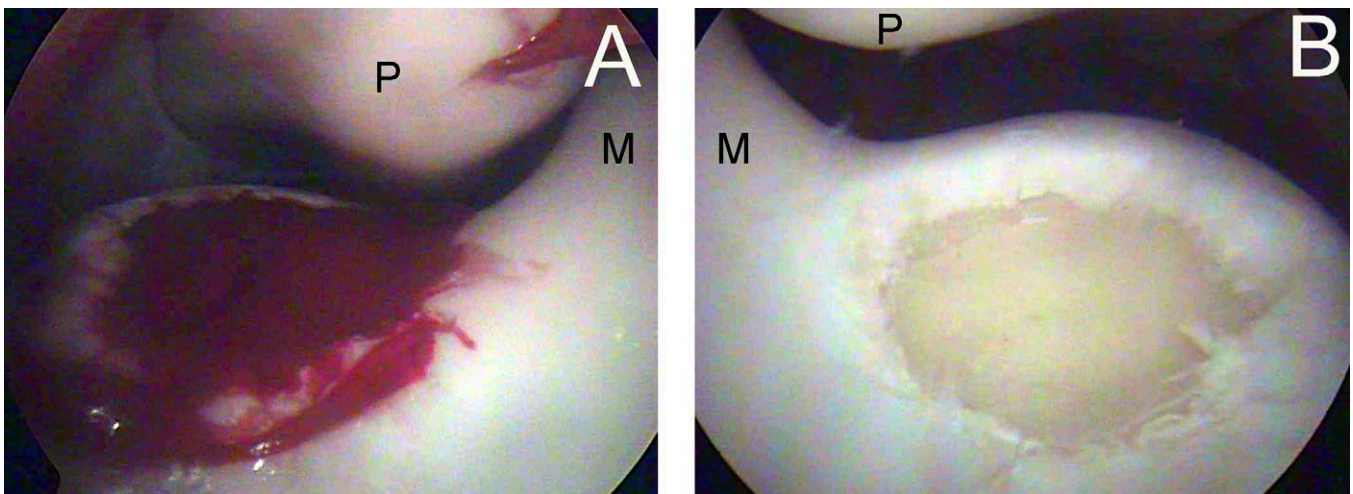

Fig. 1

Arthroscopic images of 15-mm-diameter full-thickness articular cartilage defects on the lateral trochlear ridge of the femur treated with bone marrow concentrate and microfracture (A) or with microfracture alone (B). M = medial trochlear ridge of the femur, and P = patella.

from the anesthesia had resulted in an inability to stand, and one horse was killed two months postoperatively, for humane reasons, because of a pelvic fracture that caused it pain. Second-look arthroscopy and final time-point data were available on the remaining ten horses. None of the ten remaining animals developed a joint infection or exhibited signs of lameness during the study period.

Cytological and Flow Cytometry Analyses of Bone Marrow Aspirate and Bone Marrow Concentrate

Cytological counts in the bone marrow aspirate and bone marrow concentrate are presented in Table I. The platelet count in the bone marrow concentrate was significantly increased (by 8.7-fold: 208.3 ± 192.4 [mean and standard deviation] compared with 31.1 ± 21.2 × 10^3/μL; p = 0.002) compared with that in the bone marrow aspirate. Similarly, the white blood-cell count in the bone marrow concentrate was significantly increased (by 7.4-fold: 267 ± 213 compared with 36.54 ± 16.6 × 10^3/μL; p = 0.0007) compared with that in the bone marrow aspirate. White blood-cell subpopulations were not evaluated. In contrast, the red blood-cell concentration and therefore the packed red blood-cell volume in the bone marrow concentrate were significantly decreased (by 0.5-fold: 3156 ± 1665 compared with 6774 ± 2060 × 10^3/μL; p < 0.0001) compared with that in the bone marrow aspirate. The myeloid-to-erythroid ratio, which is routinely measured in bone marrow aspirate analysis and typically used as an indicator of myeloid or erythroid dysplasia, was unchanged in the bone marrow concentrate as compared with the bone marrow aspirate and remained in the normal range (0 to 8) for horses[46] (2.09 ± 1.46 compared with 1.84 ± 0.85; p = 0.36).

Flow cytometry was performed on both bone marrow aspirate and bone marrow concentrate, but only the results for the bone marrow concentrate were obtained because of the low numbers of nucleated cells in unprocessed bone marrow aspirate. Previous flow-cytometry studies on bone marrow aspirate have suggested that mesenchymal stem cells are contained in gate 5, which is also where monocytes are found[39]. Other nucleated cells are typically distributed as follows: gates 1 and 4 contain large neutrophils, gate 2 includes lymphocytes, gate 3 contains macrophages, and gate 6 contains red blood cells and platelets[39]. Of the total nucleated cells in bone marrow concentrate, the distribution into gates was as follows: gates 1 and 4, 46.3% ± 7.8%; gate 2, 18.7% ± 6.8%; gate 3, 11.2% ± 4.2%; gate 5, 13.4% ± 3.8%; and gate 6, 3.2% ± 1.3%. Within gate 5, cells displayed the accepted profile of immunoreaction to a panel of antibodies previously suggested to help to identify mesenchymal stem cells[13,40]. Nucleated cells in gate 5 were negative for CD45 and CD34 and positive for CD44, CD29, and CD172a.

TABLE II Scores at Second-Look Arthroscopy at Twelve Weeks and Postmortem Macroscopic Assessments

	Score*		
Variable	Bone Marrow Concentrate	Microfracture	P Value
Second-look arthroscopy	6.9 ± 1.3	3.2 ± 0.9	0.002
Postmortem macroscopic appearance	9.4 ± 1.2	4.4 ± 1.2	0.009

*The values are presented as the mean and standard error of the mean. N = 10.
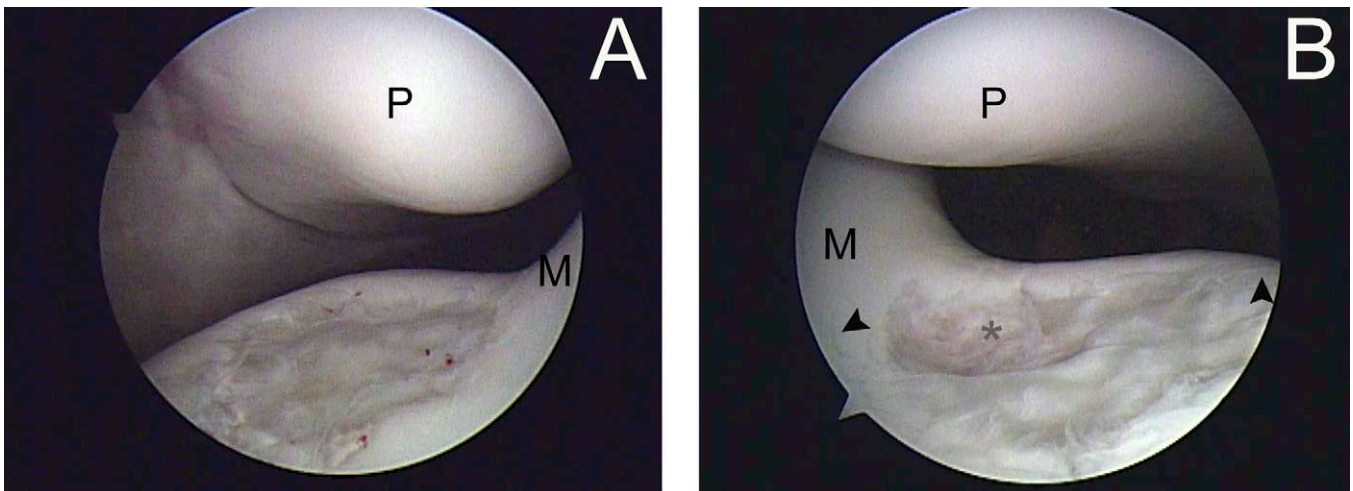

Fig. 2

Intraoperative images obtained at second-look arthroscopy at twelve weeks after treatment of cartilage defects with microfracture and bone marrow concentrate (A) or with microfracture alone (B). The arrowheads indicate full-thickness cartilage fissures, and the asterisk indicates the proximal-medial one-fourth of the defect. M = medial trochlear ridge of the femur, and P = patella.
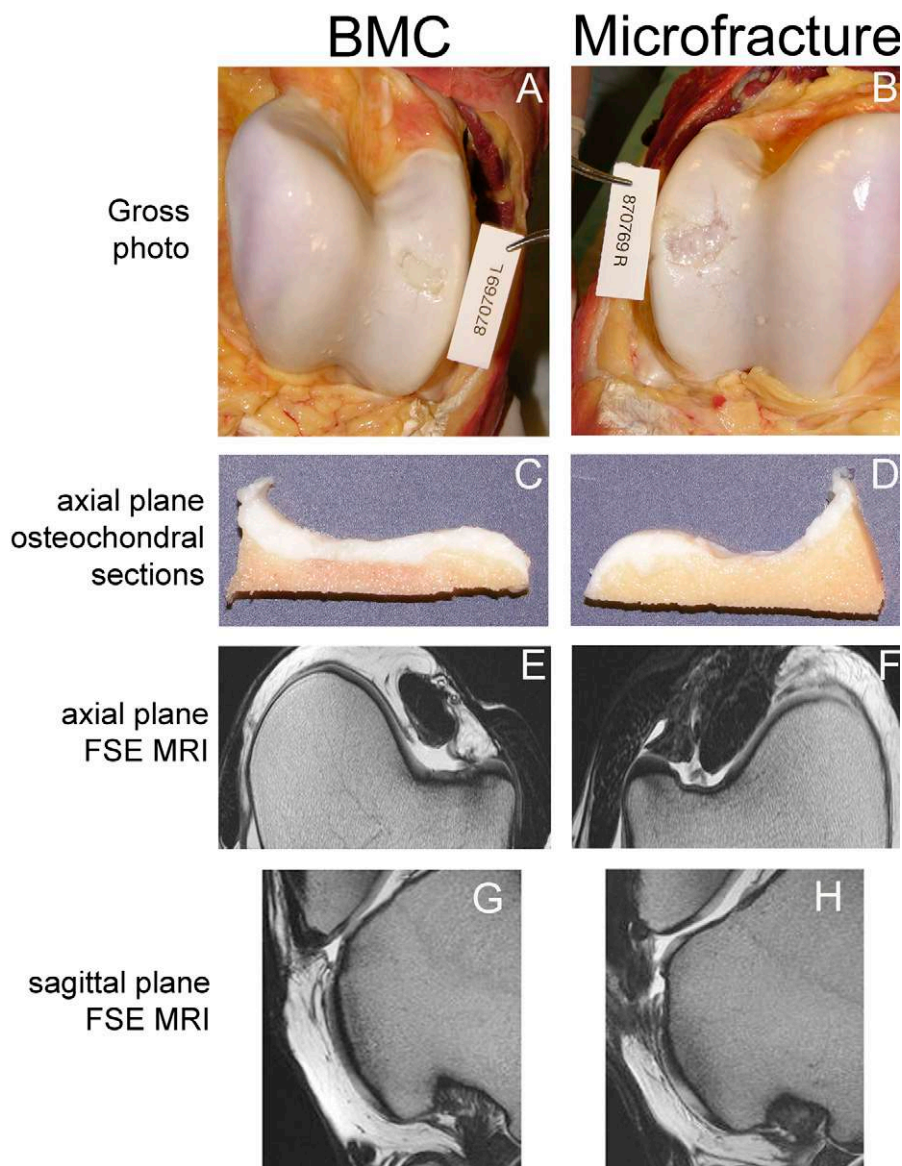
Fig. 3

Cartilage defects eight months after treatment with bone marrow concentrate (BMC; left column) or microfracture (right column). Gross photographs (A and B) and axial plane osteochondral sections (C and D) were used to generate an ICRS macroscopic assessment score. Quantitative evaluation of the repair tissue was accomplished through analysis of fast-spin-echo magnetic resonance images (FSE MRI) obtained in the axial (E and F) and sagittal (G and H) planes.

Second-Look Arthroscopic Assessment

Cartilage defects treated with bone marrow concentrate and microfracture had a significantly higher (better) ICRS score than those treated with microfracture alone (mean and standard error of the mean, 6.9 ± 1.3 compared with 3.2 ± 0.9; p = 0.002) (Fig. 2 and Table II). In addition to the variables taken into consideration in the ICRS scoring system (degree of repair, integration of the graft with the host tissue, and macroscopic appearance), the defects treated with bone marrow concentrate had no or very few (one or two) fissures radiating from their periphery, whereas the microfracture-treated defects had multiple (four, five, or six) full-thickness cartilage fissures. On the microfracture-treated sides, there was also consistently less repair tissue in the proximal-medial one-fourth of the defect (Fig. 2).

Magnetic Resonance Imaging and Macroscopic and Histological Appearance of Repair Tissue

At eight months after the surgery, the horses were killed and the patellofemoral joints were removed. The joints were subjected to magnetic resonance imaging within six to ten hours and underwent macroscopic analysis and histological sampling. On

macroscopic assessment, the defects treated with bone marrow concentrate had significantly better repair tissue than those treated with microfracture alone (mean score and standard error of the mean, 9.4 ± 1.2 compared with 4.4 ± 1.2; p = 0.009) (Table II). Treatment with bone marrow concentrate resulted in thicker, more hyaline-appearing repair tissue that visually appeared to be better integrated into the surrounding host cartilage (Fig. 3, *A*) compared with the repair tissue in the microfracture group (Fig. 3, *B*). In the microfracture-treated joints, the full-thickness fissures radiating from the periphery of the defect and the lack of fill in the proximal-medial one-fourth of the defect were still visible (Fig. 3, *B*).

Axial plane osteochondral sections removed for histological analysis supported the finding that the defects treated with bone marrow concentrate had a greater percentage of repair tissue fill than did the microfracture controls (Fig. 3, *C* and *D*). Axial and sagittal fast-spin-echo magnetic resonance imaging analysis (Fig. 3, *E* through *H*) provided quantitative validation of increased fill in the defects treated with bone marrow concentrate compared with that in the microfracture-treated defects (2.3 ± 0.32 compared with 1.2 ± 0.43; p = 0.009) (Table III). Magnetic resonance images also revealed that there were no differences in the amount of synovial reaction (0.8 ± 0.21 compared with 0.9 ± 0.24; p = 0.72), subchondral sclerosis (1.5 ± 0.23 compared with 1.3 ± 0.22; p = 0.55), or Outerbridge score in cartilage adjacent to (1 cm from) the defect or remote from the defect (medial trochlear cartilage) between the bone marrow concentrate and microfracture-treated groups (Table III). Histological analysis of the synovial membrane also re-

vealed no significant differences between the two groups (mean score, 12.7 ± 0.15 compared with 13.5 ± 0.11; p = 0.14).

Histological Analysis and Magnetic Resonance Imaging Analysis of Glycosaminoglycans and Collagen

The mean ICRS histological score for the defects treated with bone marrow concentrate was significantly better than that for the microfracture-treated defects (11.1 ± 1.6 compared with 6.4 ± 1.2; p = 0.02). In the bone marrow concentrate group, the proteoglycan staining was primarily located in the deeper layers of the repair tissue with less intense staining at the interface between the repair and surrounding host cartilage (Fig. 4, *A, B, a,* and *b*). The superficial layers of the repair tissue in the defects treated with bone marrow concentrate were also more tangentially arranged than those of the repair tissue in the microfracture group (Fig. 4, *B* and *b*). In contrast, there was negligible proteoglycan staining throughout the repair tissue in the microfracture group. Safranin O and fast green staining also revealed increased proteoglycan content in the repair tissue in the bone marrow concentrate group compared with that in the microfracture group (Fig. 5, *A* and *B*). Quantitative T1ρ mapping supported the histological observations by showing significantly increased glycosaminoglycan content in both the superficial and the deep zone within the central and peripheral regions of the repair tissue in the bone marrow concentrate group and in the deep zone of the interface between the repair and host cartilage in that group as compared with the values in the microfracture-treated, control limbs (Table IV and Fig. 5, *C* and *D*).
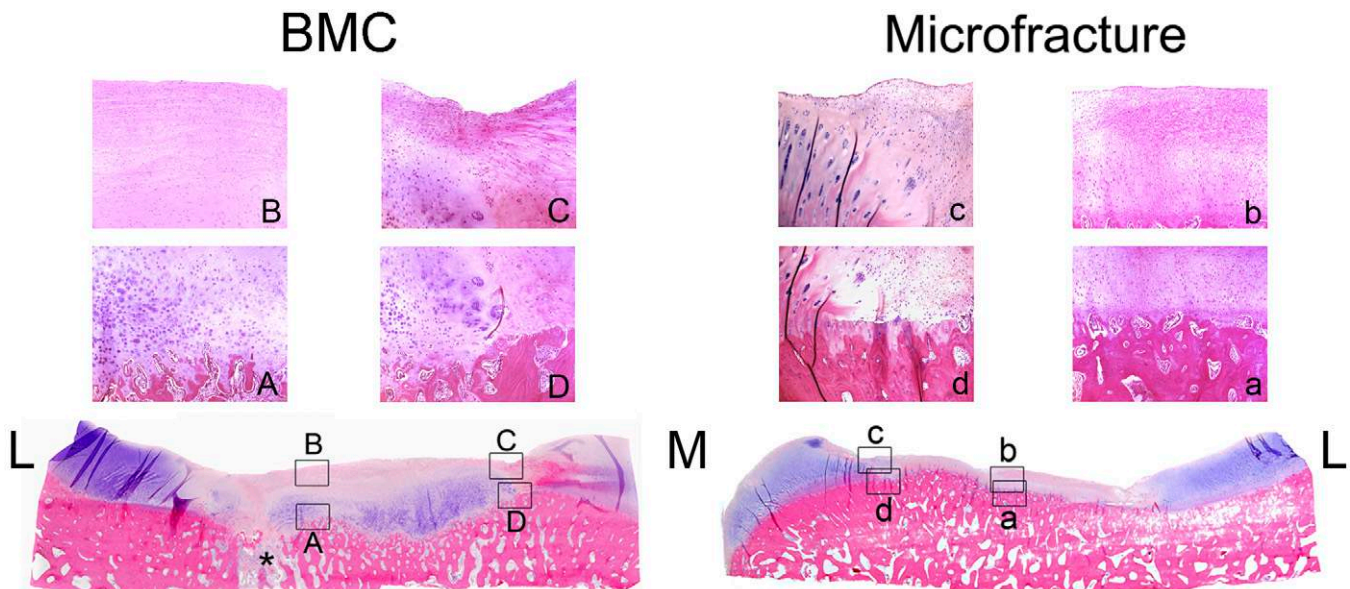

Fig. 4

Axial osteochondral sections of cartilage defects eight months after treatment with bone marrow concentrate (BMC; left panel) or microfracture (right panel). Sections were stained with hematoxylin and eosin and used to assess repair with the ICRS scoring system. Higher-magnification images (top, ×200) of the areas in the boxes in the subgross images (bottom, [0]no magnification) show repair tissue from the central deep (A, a) and central superficial (B, b) regions and from the interface junction of the repair and host cartilage in the superficial (C, c) and deep (D, d) layers. L = lateral and M = medial. The asterisk indicates a residual microfracture hole.

TABLE III Fast-Spin-Echo Magnetic Resonance Imaging Measurements Obtained Eight Months After Surgery

Variable*	Bone Marrow Concentrate†	Microfracture†	P Value
Outerbridge score			
Remote cartilage	0.5 ± 0.28	0.7 ± 0.27	0.55
Adjacent cartilage	0.7 ± 0.22	0.7 ± 0.35	1.0
% fill	2.3 ± 0.32	1.2 ± 0.43	0.009
Synovial reaction	0.8 ± 0.21	0.9 ± 0.24	0.72
Sclerosis	1.5 ± 0.23	1.3 ± 0.22	0.55

*In the Outerbridge scoring system, 0 = normal cartilage, 1 = hyperintense cartilage, 2 = <50% cartilage signal loss, 3 = >50% cartilage signal loss, and 4 = exposed subchondral bone. The remote cartilage was medial trochlear cartilage, and the adjacent cartilage was 1 cm from the defect. The percent fill was scored as 1 = <25% fill, 2 = 25% to <50% fill, 3 = 50% to 75% fill, and 4 = >75% to 100% fill. Synovial reaction and sclerosis were scored as 0 = none, 1 = mild, 2 = moderate, and 3 = severe. Synovial reaction was determined on the basis of the estimated total volume of the joint recesses. †The values are presented as the mean and standard error of the mean. N = 10.

Type-II collagen immunoreaction in the repair tissue was also greater in the bone marrow concentrate group than it was in the microfracture group (Fig. 5, E and F). In defects treated with bone marrow concentrate, the bottom 50% or more of the repair tissue was positive for type-II collagen whereas, in the microfracture-treated defects, only the very lowest layer was immunoreactive. Quantitative T2 mapping indicated improved collagen orientation in the superficial and deep zones
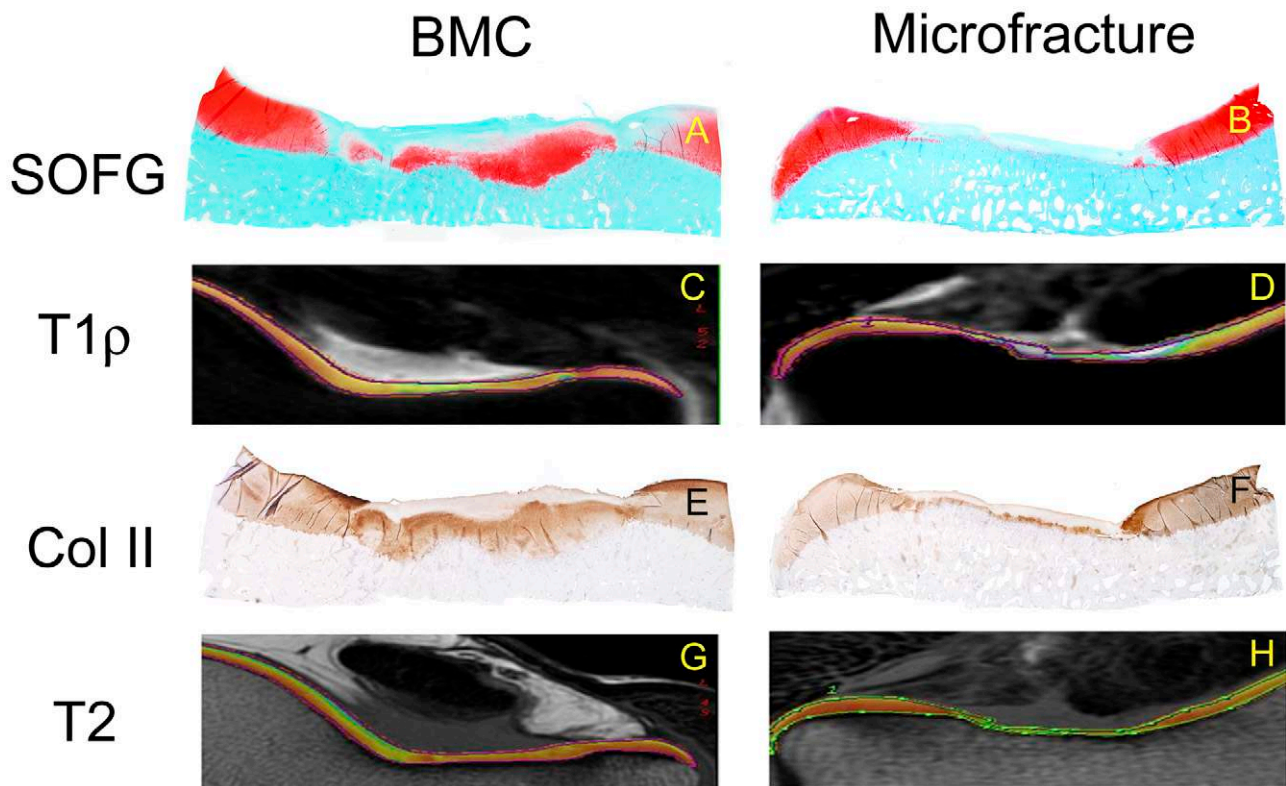

Fig. 5

Axial osteochondral sections of cartilage defects eight months after treatment with bone marrow concentrate (BMC; left column) or microfracture (right column). Repair tissue was assessed for glycosaminoglycans with use of safranin O and fast green staining (SOFG) (A and B) and quantitative magnetic resonance imaging T1ρ mapping (C and D). Collagen distribution and content were assessed with use of type-II collagen immunohistochemistry (Col II) (E and F), and collagen orientation was evaluated with quantitative magnetic resonance imaging T2 mapping (G and H).

TABLE IV Results of Quantitative Magnetic Resonance Imaging Mapping Obtained Eight Months After Surgery

Region of Interest/Zone*	T1ρ Mapping†		T2 Mapping†	
	Bone Marrow Concentrate	Microfracture	Bone Marrow Concentrate	Control
Central				
Superficial zone	110.1 ± 12.2‡	142.2 ± 12.4	31.8 ± 2.2‡	46.1 ± 4.1
Deep zone	93.8 ± 9.5‡	124.4 ± 12.4	27.1 ± 2.3‡	38.5 ± 2.7
Peripheral				
Superficial zone	93.7 ± 6.8‡	125.4 ± 12.5	30.4 ± 3.0‡	48.1 ± 4.2
Deep zone	83.7 ± 4.1‡	118.2 ± 9.2	26.5 ± 2.5‡	42.3 ± 4.9
Interface				
Superficial zone	105.0 ± 6.9	119.6 ± 35.8	43.0 ± 2.9‡	64.1 ± 4.3
Deep zone	98.9 ± 6.3‡	158.4 ± 54.6	21.2 ± 3.2‡	48.8 ± 1.9
Adjacent				
Superficial zone	90.1 ± 5.8	93.0 ± 6.8	39.2 ± 1.9	36.9 ± 2.9
Deep zone	79.1 ± 6.2	76.7 ± 6.6	17.0 ± 1.2	17.4 ± 1.4
Remote (native cartilage)				
Superficial zone	84.4 ± 5.2	84.9 ± 1.9	35.1 ± 2.8	37.3 ± 2.2
Deep zone	67.2 ± 4.6	65.7 ± 2.2	17.0 ± 1.1	17.8 ± 1.7

*The regions of interest were the central repair tissue, peripheral repair tissue, interface of the repair tissue and the host cartilage, adjacent cartilage (1 cm from the defect), and remote (medial trochlear) cartilage. Measurements were obtained in superficial and deep layers within each region of interest. †The values are presented as the mean and standard error of the mean in milliseconds. N = 10. ‡There was a significant difference between the bone marrow concentrate and microfracture groups (p < 0.05).

within the central, peripheral, and interface regions of bone marrow concentrate repair tissues compared with that in the microfracture-treated defects (Table IV and Fig. 5, *G* and *H*).

Discussion

In this study, the addition of bone marrow concentrate resulted in significantly improved cartilage repair compared with that following microfracture; this was demonstrated with use of both short-term arthroscopic assessment and longer-term macroscopic, histological, and quantitative magnetic resonance imaging analyses. The differences between the bone marrow concentrate and microfracture groups observed arthroscopically at twelve weeks persisted at the eight-month evaluation. In particular, the repair tissue in the defects treated with bone marrow concentrate was much better integrated into the surrounding normal cartilage, the tissue was thicker, and the tissue had a smoother surface. A consistent deficiency in the repair tissue was noted in the proximal-medial aspect of the microfracture-treated defects. In large (15-mm-diameter) cartilage defects in the lateral trochlear ridge of the femur, spontaneous healing is more apparent distally than it is proximally[47], so it was not surprising to find that the more proximal aspect of the defect was filled with less repair tissue on the microfracture-treated side. Of note is the fact that this topographical discrepancy in the extent of repair was not apparent in the bone marrow concentrate-treated defects, in which repair was consistent throughout.

The subchondral bone on the defects treated with bone marrow concentrate was subjected to microfracture prior to bone marrow concentrate grafting. The purpose of the microfracture prior to the treatment with the bone marrow concentrate was to produce roughened areas for the base of the bone marrow concentrate graft to increase graft security. Microfracture was performed under helium arthroscopy, and the subchondral bed was dried prior to implantation of the bone marrow concentrate, so it is unlikely that bleeding from the microfracture holes appreciably contributed to the composition of the bone marrow concentrate clot. Long-term consequences of microfracture and other marrow-stimulation techniques, such as an increased rate of failure of subsequent autologous chondrocyte implantation, have been reported[48], and alternative methods to enhance the security of the bone marrow concentrate clot should be considered. The long-term durability of the results of microfracture has been questioned, but it was chosen as the comparison group since it is considered by many as the first-line treatment for cartilage defects[4,7,8] and because microfracture was performed prior to implantation of the bone marrow concentrate.

For this equine model of an extensive cartilage defect, eight months appears to be an adequate duration of follow-up to allow maturation or deterioration of early repair tissue and to permit evaluation of cartilage repair[12,49-51]. In the present study, bone marrow concentrate grafting resulted in an improved arthroscopic appearance of the repair tissue at three

months, and the repair tissue remained significantly improved at eight months. However, longer-term data and an evaluation of the return to athletic performance would be required to determine the ultimate durability of the repair tissue following treatment with bone marrow concentrate. In this study, the acute cartilage defects were made in normal joints, so the investigation did not provide information regarding the ability of bone marrow concentrate grafting to result in resolution of clinical symptoms.

Cytological analyses of the bone marrow concentrate suggested that centrifugation of bone marrow aspirate results in significant concentration of platelets and white blood cells and a decrease in red blood cells. Although growth factors were not quantified in this study, there is a strong positive correlation between platelets and anabolic growth factors such as PDGF and TGF-β in equine platelet-rich plasma[16]. Flow cytometry suggests that there are cells that display cell surface markers consistent with mesenchymal stem cells, but the exact quantity of stem cells cannot be measured with these methods since there is no cell-surface-marker profile that is specific for bone marrow-derived stem cells. Furthermore, recent studies suggest that cell surface markers on nucleated cells in fresh bone marrow aspirate and bone marrow concentrate differ from those on cultured cells, leading to further difficulties with attempts to quantify stem cells in a suspension[39]. It would be interesting to quantify the exact number of stem cells in the bone marrow concentrate in order to determine if stem-cell quantity was related to the quality of the repair tissue since the role of stem cells in tissue regeneration remains unclear[11]. In addition to stem cells and growth factors released from platelets, the presence of a three-dimensional structural support for the graft and the surrounding host cartilage likely contributed to the improved repair in the defects treated with bone marrow concentrate. Although understanding the independent contributions of stem cells, growth factors, or scaffolds to new cartilage formation was not an objective of the present study, their combination in a one-step, autogenous, arthroscopically applied method resulted in enhanced cartilage regeneration.

The use of 3-T magnetic resonance mapping in this study provided quantitative validation of macroscopic and histological scores. The immunohistochemistry results indicated increased type-II collagen in the repair tissue in the bone marrow concentrate group, and magnetic resonance T2 mapping revealed that the collagen orientation in the repair tissue in that group more closely approximated normal cartilage than did the repair tissue found in the microfracture-treated defects. Similarly, histological analysis indicated a significant increase in matrix glycosaminoglycan, which was verified through magnetic resonance T1ρ mapping. Together, these results indicate that bone marrow concentrate results in significant improvements in both biochemical and structural components of the cartilage repair matrix. Clinical studies are needed to determine the ability of bone marrow concentrate grafting to relieve clinical symptoms and to determine the long-term durability of the repair tissue that is formed. ∎

Lisa A. Fortier, DVM, PhD
Lauren V. Schnabel, DVM
Tracy Stokol, BVSc, PhD
Jon Cheetham, VetMB, PhD
Alan J. Nixon, BVSc, MS
Departments of Clinical Sciences (L.A.F., L.V.S., J.C., and A.J.N.)
and Population Medicine and Diagnostic Sciences (T.S.),
VMC C3-181, Cornell University, Ithaca, NY 14853.
E-mail address for L.A. Fortier: laf4@cornell.edu

Hollis G. Potter, MD
Li Foong Foo, MD
Leroy R. Chong, MD
MRI Division, Hospital for Special Surgery,
535 East 70th Street,
New York, NY 10021

Ellen J. Rickey, DVM
University of Guelph,
50 Stone Road, Guelph,
ON N1G 2W1, Canada

References

1. Widuchowski W, Widuchowski J, Trzaska T. Articular cartilage defects: study of 25,124 knee arthroscopies. Knee. 2007;14:177-82.

2. Hjelle K, Solheim E, Strand T, Muri R, Brittberg M. Articular cartilage defects in 1,000 knee arthroscopies. Arthroscopy. 2002;18:730-4.

3. McNickle AG, Provencher MT, Cole BJ. Overview of existing cartilage repair technology. Sports Med Arthrosc. 2008;16:196-201.

4. Magnussen RA, Dunn WR, Carey JL, Spindler KP. Treatment of focal articular cartilage defects in the knee: a systematic review. Clin Orthop Relat Res. 2008;466:952-62.

5. Stoddart MJ, Grad S, Eglin D, Alini M. Cells and biomaterials in cartilage tissue engineering. Regen Med. 2009;4:81-98.

6. Goldring MB, Otero M, Tsuchimochi K, Ijiri K, Li Y. Defining the roles of inflammatory and anabolic cytokines in cartilage metabolism. Ann Rheum Dis. 2008;67 Suppl 3:iii75-82.

7. Mithoefer K, McAdams T, Williams RJ, Kreuz PC, Mandelbaum BR. Clinical efficacy of the microfracture technique for articular cartilage repair in the knee: an evidence-based systematic analysis. Am J Sports Med. 2009;37:2053-63.

8. Gill TJ, McCulloch PC, Glasson SS, Blanchet T, Morris EA. Chondral defect repair after the microfracture procedure: a nonhuman primate model. Am J Sports Med. 2005;33:680-5.

9. Wakitani S, Saito T, Caplan AI. Myogenic cells derived from rat bone marrow mesenchymal stem cells exposed to 5-azacytidine. Muscle Nerve. 1995;18:1417-26.

10. Fortier LA, Nixon AJ, Williams J, Cable CS. Isolation and chondrocytic differentiation of equine bone marrow-derived mesenchymal stem cells. Am J Vet Res. 1998;59:1182-7.

11. Chen FH, Tuan RS. Mesenchymal stem cells in arthritic diseases. Arthritis Res Ther. 2008;10:223.

12. Wilke MM, Nydam DV, Nixon AJ. Enhanced early chondrogenesis in articular defects following arthroscopic mesenchymal stem cell implantation in an equine model. J Orthop Res. 2007;25:913-25.

CONCENTRATED BONE MARROW ASPIRATE IMPROVES
FULL-THICKNESS CARTILAGE REPAIR

13. Pittenger MF, Mackay AM, Beck SC, Jaiswal RK, Douglas R, Mosca JD, Moorman MA, Simonetti DW, Craig S, Marshak DR. Multilineage potential of adult human mesenchymal stem cells. Science. 1999;284:143-7.

14. Martin DR, Cox NR, Hathcock TL, Niemeyer GP, Baker HJ. Isolation and characterization of multipotential mesenchymal stem cells from feline bone marrow. Exp Hematol. 2002;30:879-86.

15. Schnabel LV, Mohammed HO, Miller BJ, McDermott WG, Jacobson MS, Santangelo KS, Fortier LA. Platelet rich plasma (PRP) enhances anabolic gene expression patterns in flexor digitorum superficialis tendons. J Orthop Res. 2007; 25:230-40.

16. McCarrel T, Fortier L. Temporal growth factor release from platelet-rich plasma, trehalose lyophilized platelets, and bone marrow aspirate and their effect on tendon and ligament gene expression. J Orthop Res. 2009;27:1033-42.

17. Potier E, Ferreira E, Dennler S, Mauviel A, Oudina K, Logeart-Avramoglou D, Petite H. Desferrioxamine-driven upregulation of angiogenic factor expression by human bone marrow stromal cells. J Tissue Eng Regen Med. 2008;2:272-8.

18. Mehta S, Watson JT. Platelet rich concentrate: basic science and current clinical applications. J Orthop Trauma. 2008;22:432-8.

19. Huang AH, Motlekar NA, Stein A, Diamond SL, Shore EM, Mauck RL. High-throughput screening for modulators of mesenchymal stem cell chondrogenesis. Ann Biomed Eng. 2008;36:1909-21.

20. Indrawattana N, Chen G, Tadokoro M, Shann LH, Ohgushi H, Tateishi T, Tanaka J, Bunyaratvej A. Growth factor combination for chondrogenic induction from human mesenchymal stem cell. Biochem Biophys Res Commun. 2004;320:914-9.

21. Johnstone B, Hering TM, Caplan AI, Goldberg VM, Yoo JU. In vitro chondrogenesis of bone marrow-derived mesenchymal progenitor cells. Exp Cell Res. 1998;238:265-72.

22. Murdoch AD, Grady LM, Ablett MP, Katopodi T, Meadows RS, Hardingham TE. Chondrogenic differentiation of human bone marrow stem cells in transwell cultures: generation of scaffold-free cartilage. Stem Cells. 2007;25:2786-96.

23. Mishra A, Tummala P, King A, Lee B, Kraus M, Tse V, Jacobs CR. Buffered platelet-rich plasma enhances mesenchymal stem cell proliferation and chondrogenic differentiation. Tissue Eng Part C Methods. 2009;15:431-5.

24. Huang Q, Wang YD, Wu T, Jiang S, Hu YL, Pei GX. Preliminary separation of the growth factors in platelet-rich plasma: effects on the proliferation of human marrow-derived mesenchymal stem cells. Chin Med J (Engl). 2009;122:83-7.

25. Dickhut A, Gottwald E, Steck E, Heisel C, Richter W. Chondrogenesis of mesenchymal stem cells in gel-like biomaterials in vitro and in vivo. Front Biosci. 2008;13:4517-28.

26. Goodrich LR, Nixon AJ, Fubini SL, Ducharme NG, Fortier LA, Warnick LD, Ludders JW. Epidural morphine and detomidine decreases postoperative hindlimb lameness in horses after bilateral stifle arthroscopy. Vet Surg. 2002;31:232-9.

27. van den Borne MP, Raijmakers NJ, Vanlauwe J, Victor J, de Jong SN, Bellemans J, Saris DB; International Cartilage Repair Society. International Cartilage Repair Society (ICRS) and Oswestry macroscopic cartilage evaluation scores validated for use in Autologous Chondrocyte Implantation (ACI) and microfracture. Osteoarthritis Cartilage. 2007;15:1397-402.

28. Peterson L, Minas T, Brittberg M, Nilsson A, Sjögren-Jansson E, Lindahl A. Two-to 9-year outcome after autologous chondrocyte transplantation of the knee. Clin Orthop Relat Res. 2000;374:212-34.

29. Smith GD, Taylor J, Almqvist KF, Erggelet C, Knutsen G, Garcia Portabella M, Smith T, Richardson JB. Arthroscopic assessment of cartilage repair: a validation study of 2 scoring systems. Arthroscopy. 2005;21:1462-7.

30. Kelly BT, Robertson W, Potter HG, Deng XH, Turner AS, Lyman S, Warren RF, Rodeo SA. Hydrogel meniscal replacement in the sheep knee: preliminary evaluation of chondroprotective effects. Am J Sports Med. 2007;35:43-52.

31. Mithoefer K, Williams RJ 3rd, Warren RF, Potter HG, Spock CR, Jones EC, Wickiewicz TL, Marx RG. Chondral resurfacing of articular cartilage defects in the knee with the microfracture technique. Surgical technique. J Bone Joint Surg Am. 2006;88 Suppl 1(Pt 2):294-304.

32. Glenn RE Jr, McCarty EC, Potter HG, Juliao SF, Gordon JD, Spindler KP. Comparison of fresh osteochondral autografts and allografts: a canine model. Am J Sports Med. 2006;34:1084-93.

33. Potter HG, Black BR, Chong le R. New techniques in articular cartilage imaging. Clin Sports Med. 2009;28:77-94.

34. Choi YS, Potter HG, Chun TJ. MR imaging of cartilage repair in the knee and ankle. Radiographics. 2008;28:1043-59.

35. Li X, Benjamin Ma C, Link TM, Castillo DD, Blumenkrantz G, Lozano J, Carballido-Gamio J, Ries M, Majumdar S. In vivo T(1rho) and T(2) mapping of articular cartilage in osteoarthritis of the knee using 3 T MRI. Osteoarthritis Cartilage. 2007;15: 789-97.

36. Potter HG, Chong le R. Magnetic resonance imaging assessment of chondral lesions and repair. J Bone Joint Surg Am. 2009;91 Suppl 1:126-31.

37. Mainil-Varlet P, Aigner T, Brittberg M, Bullough P, Hollander A, Hunziker E, Kandel R, Nehrer S, Pritzker K, Roberts S, Stauffer E; International Cartilage Repair Society. Histological assessment of cartilage repair: a report by the Histology End-point Committee of the International Cartilage Repair Society (ICRS). J Bone Joint Surg Am. 2003;85 Suppl 2:45-57.

38. Flaminio MJ, Yen A, Antczak DF. The proliferation inhibitory proteins p27(Kip1) and retinoblastoma are involved in the control of equine lymphocyte proliferation. Vet Immunol Immunopathol. 2004;102:363-77.

39. Radcliffe CH, Flaminio MJ, Fortier LA. Temporal analysis of equine bone marrow aspirate during establishment of putative mesenchymal progenitor cell populations. Stem Cells Dev. 2010;19:269-82.

40. Dominici M, Le Blanc K, Mueller I, Slaper-Cortenbach I, Marini F, Krause D, Deans R, Keating A, Prockop Dj, Horwitz E. Minimal criteria for defining multipotent mesenchymal stromal cells. The International Society for Cellular Therapy position statement. Cytotherapy. 2006;8:315-7.

41. Kelly BT, Potter HG, Deng XH, Pearle AD, Turner AS, Warren RF, Rodeo SA. Meniscal allograft transplantation in the sheep knee: evaluation of chondroprotective effects. Am J Sports Med. 2006;34:1464-77.

42. Li X, Han ET, Busse RF, Majumdar S. In vivo T(1rho) mapping in cartilage using 3D magnetization-prepared angle-modulated partitioned k-space spoiled gradient echo snapshots (3D MAPSS). Magn Reson Med. 2008;59:298-307.

43. Maier CF, Tan SG, Hariharan H, Potter HG. T2 quantitation of articular cartilage at 1.5 T. J Magn Reson Imaging. 2003;17:358-64.

44. Outerbridge RE. The etiology of chondromalacia patellae. J Bone Joint Surg Br. 1961;43:752-7.

45. Rosenberg L. Chemical basis for the histological use of safranin O in the study of articular cartilage. J Bone Joint Surg Am. 1971;53:69-82.

46. Malikides N, Kessell A, Hodgson JL, Rose RJ, Hodgson DR. Bone marrow response to large volume blood collection in the horse. Res Vet Sci. 1999;67: 285-93.

47. Fortier LA, Balkman CE, Sandell LJ, Ratcliffe A, Nixon AJ. Insulin-like growth factor-I gene expression patterns during spontaneous repair of acute articular cartilage injury. J Orthop Res. 2001;19:720-8.

48. Minas T, Gomoll AH, Rosenberger R, Royce RO, Bryant T. Increased failure rate of autologous chondrocyte implantation after previous treatment with marrow stimulation techniques. Am J Sports Med. 2009;37:902-8.

49. Goodrich LR, Hidaka C, Robbins PD, Evans CH, Nixon AJ. Genetic modification of chondrocytes with insulin-like growth factor-1 enhances cartilage healing in an equine model. J Bone Joint Surg Br. 2007;89:672-85.

50. Fortier LA, Mohammed HO, Lust G, Nixon AJ. Insulin-like growth factor-I enhances cell-based repair of articular cartilage. J Bone Joint Surg Br. 2002;84: 276-88.

51. Hidaka C, Goodrich LR, Chen C-T, Warren RF, Crystal RG, Nixon AJ. Acceleration of cartilage repair by genetically modified chondrocytes over expressing bone morphogenetic protein-7. J Orthop Res. 2003;21:573-83.